ELSEVIER

Tectonophysics 351 (2002) 119–137

TECTONOPHYSICS

www.elsevier.com/locate/tecto

Paleomagnetic study of Cenozoic sediments from the Zaisan basin (SE Kazakhstan) and the Chuya depression (Siberian Altai): tectonic implications for central Asia

J.C. Thomas [a,*], R. Lanza [b], A. Kazansky [c], V. Zykin [c], N. Semakov [c], D. Mitrokhin [c], D. Delvaux [d]

[a] *Laboratoire de Géophysique interne et Tectonophysique, CNRS UMR 5654, BP 53X, 38000 Grenoble, France*
[b] *Dipartimento di Scienze della Terra, Università di Torino, via Valperga Caluso 35, 10125 Turin, Italy*
[c] *United Institute of Geology, Geophysics, and Mineralogy, SB RAS, Novosibirsk, Russia*
[d] *Royal Museum for Central Africa, Tervuren, Belgium*

Abstract

This paper presents new paleomagnetic results on Cenozoic rocks from northern central Asia. Eighteen sites were sampled in Pliocene to Miocene clays and sandy clays of the Zaisan basin (southeastern Kazakhstan) and 12 sites in the upper Oligocene to Pleistocene clays and sandstones of the Chuya depression (Siberian Altai). Thermal demagnetization of isothermal remanent magnetization (IRM) showed that hematite and magnetite are the main ferromagnetic minerals in the deposits of the Zaisan basin. Stepwise thermal demagnetization up to 640–660 °C isolated a characteristic (ChRM) component of either normal or reverse polarity at nine sites. At two other sites, the great circles convergence method yielded a definite direction. Measurements of the anisotropy of magnetic susceptibility showed that the hematite-bearing sediments preserved their depositional fabric. These results suggest a primary origin of the ChRM and were substantiated by positive fold and reversal tests. The mean paleomagnetic direction for the Zaisan basin ($D=9°$, $I=59°$, $k=19$, $\alpha_{95}=11°$) is close to the expected direction derived from the APW path of Eurasia [J. Geophys. Res. 96 (1991) 4029] and shows that the basin did not rotated relative to stable Asia during the Tertiary. In the upper Pliocene–Pleistocene sandstones of the Chuya depression, a very stable ChRM carried by hematite was found. Its mean direction ($D=9°$, $I=46°$, $k=25$, $\alpha_{95}=7°$) is characterized by declination close to the one excepted for early Quaternary, whereas inclination is lower. In the middle Miocene to lower Pliocene clays and sandstones, a stable ChRM of both normal and reverse polarities carried by magnetite was isolated. Its mean direction ($D=332°$, $I=63°$, $k=31$, $\alpha_{95}=4°$) is deviated with respect to the reference direction and implies a Neogene, $39 \pm 8°$ counterclockwise rotation of the Chuya depression relative to stable Asia. These results and those from the literature suggest that the different amount of rotation found in the two basins is related to a sharp variation in their tectonic style, predominantly compressive in the Zaisan basin and transpressive in the Siberian Altai. At a larger scale, the pattern of vertical axis rotations deduced from paleomagnetic data in northern central Asia is consistent with the hypothesis of a large left-lateral shear zone running from the Pamirs to the Baikal. Heterogeneous rotations, however, indicate changes in style of faulting along the shear zone and local effect for the domains with the largest rotations.

Keywords: Cenozoic; Northern central Asia; Paleomagnetism; Tectonic rotation

* Corresponding author. Tel.: +33-4-766-35683; fax: +33-4-768-28101.
E-mail address: jean-charles.thomas@obs.ujf-grenoble.fr (J.C. Thomas).

0040-1951/02/$ - see front matter
PII: S0040-1951(02)00128-2

1. Introduction

In central Asia, strong intracontinental deformation related to the collision of India with Asia has occurred for 45 million years (Molnar and Tapponnier, 1975). The 2000 km of convergence have been accommodated by thickening, large horizontal displacement along strike-slip faults and vertical axis rotation (Molnar and Tapponnier, 1975; Cobbold and Davy, 1988; Dewey et al., 1989; England and Molnar, 1990). However, the actual contribution of each mechanism is still controversial. Some hypotheses support thickening as the dominant mechanism in Tibet and Tien-Shan (Houseman and England, 1986, 1993; Dewey et al., 1989; Searle, 1996), while others favor eastward extrusion of crustal blocks along major strike-slip faults (Tapponnier et al., 1986; Avouac et al., 1993). Block rotation about vertical axes has also been inferred as a substantial mechanism in regions where wrenching is important (Cobbold and Davy, 1988; England and Molnar, 1990; Bayasgalan et al., 1999) (Fig. 1):

(1) In the eastern Himalayan syntaxis, the northward displacement of the Tibet relative to eastern China has been accommodated by right lateral wrenching and clockwise block rotation.

(2) In a strip running from the Pamirs to the Baikal, the westward extrusion of mobile Asia relatively to stable Asia has induced left-lateral wrenching and counterclockwise rotation of blocks bounded by antithetic right-lateral strike-slip faults. Within the strip, left-lateral transpression has occurred in the Tien-Shan and the Altai and left-lateral transtension in the Baikal region and eastern Mongolia (Cobbold and Davy, 1988; Cunningham, 1998).

Paleomagnetic studies have demonstrated that substantial vertical axis rotations have occurred in eastern Tibet (Huang and Opdike, 1992; Funahara et al., 1992) and in the Tien-Shan range (Thomas et al., 1993, 1994). In some regions, however, the need for paleomagnetic data remains crucial to better constrain the pattern of Tertiary rotations and kinematics of central Asia. In this paper, we present new Tertiary paleomagnetic data from two regions located in the central part of the Pamirs–Baikal strip (Fig. 1): the Zaisan basin of southeastern Kazakhstan and the Chuya depression in the Siberian Altai range.

2. Tectonic setting

The Altai consists of a succession of NW–SE ranges up to 4500 m high alternating with intermountain compressive basins filled with Mesozoic and Cenozoic detrital sediments. The Cenozoic style of deformation is dominated by transpression. Right-lateral transpression produced in the Mongolian Altai large-scale positive flower structures oriented NW–SE (Cunningham et al., 1996a,b). In these structures, the faults that bound the basins (i.e. Fu-Yun fault, Hars Us Nuur fault) show a combination of right-lateral strike-slip and reverse displacement. Flower structures oriented E–W to N110° and evolving in a left-lateral strike-slip context occur to the southeast, in the Gobi Altai (Cunningham et al., 1997), and also to the northwest, in the Siberian Altai, where the Chuya depression is located (Fig. 1). The Chuya depression is one of the few intermountain compressive basins of the area (Delvaux et al., 1995) and the only one where a continuous Cenozoic sedimentary sequence crops out. Structural data show that, after an extensional phase during the middle Oligocene, the depression developed in a left-lateral transpressive context (Delvaux et al., 1995, submitted for publication).

Southwest of the Altai range lie the Junggar (northwestern China) and the Zaisan (southeastern Kazakhstan) basins (Fig. 1). The Fu-Yun right-lateral strike-slip fault marks a sharp boundary between the Junggar basin and the Altai range in China (Tapponnier and Molnar, 1979). To the northwest, in Kazakhstan, the Altai range is separated from the Kazakh platform by the Irtysh shear zone, which formed in late Paleozoic as a result of left-lateral strike-slip movements between the Siberian (including the Altai range) and the Kazakhstan–Junggar plates during late Paleozoic (Allen et al., 1995), and was reactivated by right-lateral transpression in late Cenozoic (Delvaux et al., submitted for publication). This strike-slip boundary is an important fault system composed of several parallel segments extending up to the western Siberian plain and separates the Siberian Altai from the Zaisan basin. This is a large compressive basin filled by upper Paleozoic to Cenozoic sediments with a thickness of up to 6 km (Mekhed and Chamikov, 1987). It is bounded to the southwest by reverse faults, to the northeast by the

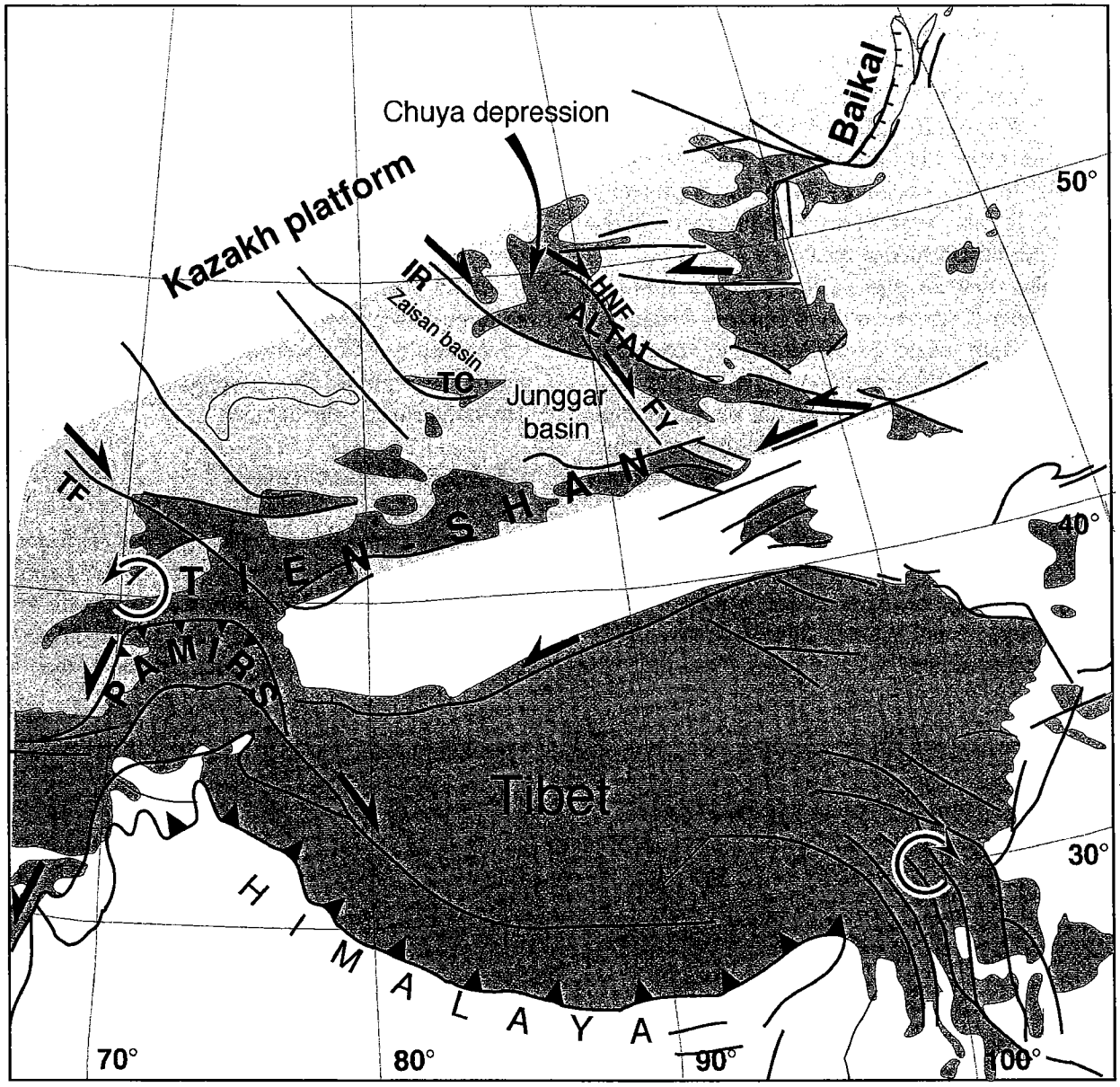

Fig. 1. Tectonic sketch map of central Asia with major Cenozoic faults. Symbols: dark grey/white = elevation above/below 2000 m; light grey = Pamirs–Baikal wrenching strip; BF = Bolnai fault, FY = Fu-Yun fault; HNF = Hars–Us–Nuur fault; IR = Irtysh fault zone; TC = Tarbagatay–Chingiz range; TF = Talass–Fergana fault.

Irtysh shear zone and separated from the Junggar basin by the Tarbagatay–Chingiz range. Except for the Irtysh/Fu-Yun fault zone, deformation style in the Junggar and in the Zaisan basins is dominantly compressional (Tapponnier and Molnar, 1979; Avouac et al., 1993; Delvaux et al., submitted for publication).

3. Paleomagnetism of the Zaisan basin

3.1. Stratigraphy and sampling

An upper Cretaceous–Cenozoic sequence occurs in the central part of the Zaisan basin with a maximum thickness of up to 1800 m close to the southern

border. Sediments essentially consist of clays and sandy clays (Erofiev, 1960; Vasilenko, 1961; Borisov, 1963). A narrow strip of Paleozoic rocks in low hills oriented E–W to N110° (Fig. 2) divides the basin in two parts. A Cenozoic fault running along the hills and parallel to the margins of the basin is probably responsible for the separation. Paleomagnetic sampling was performed in two areas:

(1) In the northern part of the basin, a strongly reduced Upper Cretaceous to Cenozoic sequence occurs, essentially made up of Paleogene and lower Neogene sediments reaching up to 500 m in thickness. Well-exposed sediments are lying flat or gently dipping to the SW and unconformably lie over an upper Paleozoic basement. Five sites were sampled at the Karabirŏk locality in Paleocene clays (site Kara5) and upper to lower Eocene clays and sandy clays (sites Kara1, 2, 3, 4) (Erofiev, 1960). These last units were also sampled at sites Acho1, 2, 3 and Acho5, 6 while Oligocene clays of the Achotas suite (Borisov, 1963) were sampled at Acho4.

(2) In the southeastern part of the basin, the Cenozoic rocks are folded parallel to the basin margin. During late Quaternary, this margin was uplifted with respect to the central part and deep erosion provided good outcrops of the folded Cenozoic sequence. Paleocene to lower Miocene light red to brown sandy clays and clays (Borisov, 1963) were sampled at seven sites along or close to the Kalmakpay River.

About 200 specimens were drilled with a portable, gasoline-powered equipment and a few were taken as hand-samples. They were oriented with both magnetic and sun compass. We observed a mean magnetic declination of 6° for the area.

3.2. Magnetic measurements

Natural remanent magnetization (NRM) was measured with JR-4 and JR-5 spinners, while susceptibility and its anisotropy (AMS) were measured with a KLY-2 bridge. Demagnetization of pilot specimens showed that thermal treatment was more effective than alter-

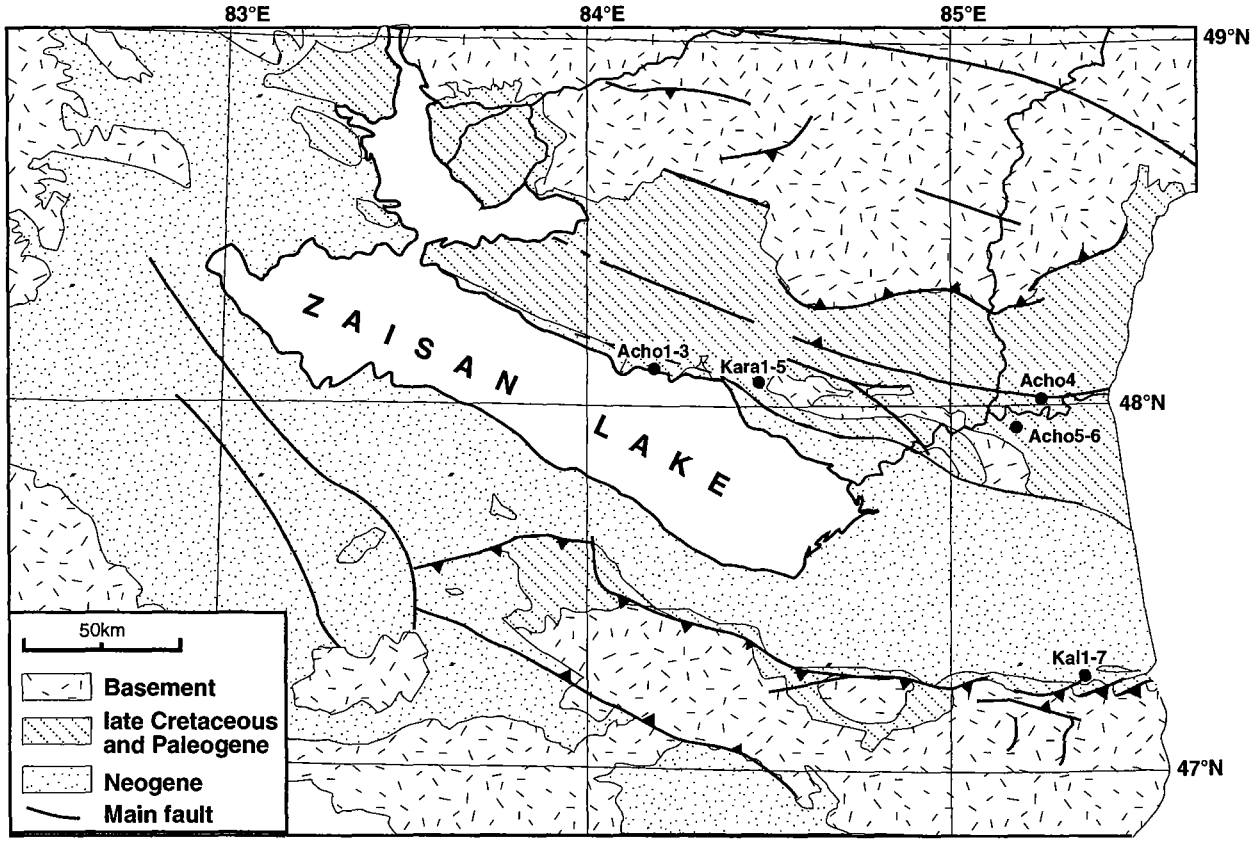

Fig. 2. Geological sketch map of the Zaisan basin and location of sampling sites.

nating field (AF) in isolating characteristic components (ChRM). All specimens were therefore thermally demagnetized at 6 to 10 steps using a Schonstedt TSD1. Magnetic mineralogy was analyzed for at least one specimen per site by thermal demagnetization of isothermal remanent magnetization (IRM) (Lowrie, 1990), measuring three mutually orthogonal components acquired in fields of 1.5, 0.5 and 0.1 T, respectively.

3.2.1. Northern part of the basin

Both in Karabirok and Achotas, the sites could be divided into two groups according to the widely different magnetic properties of rocks. The first group (Kara3, 5 and Acho4, 5, 6) was characterized by susceptibility values $200 < k < 900 \times 10^{-6}$ SI and NRM intensity $J_r > 1 \times 10^{-3}$ A/m. The second group (Kara1, 2, 4 and Acho1, 2, 3) displayed lower values, $20 < k < 150 \times 10^{-6}$ SI and $J_r < 5 \times 10^{-4}$ A/m,

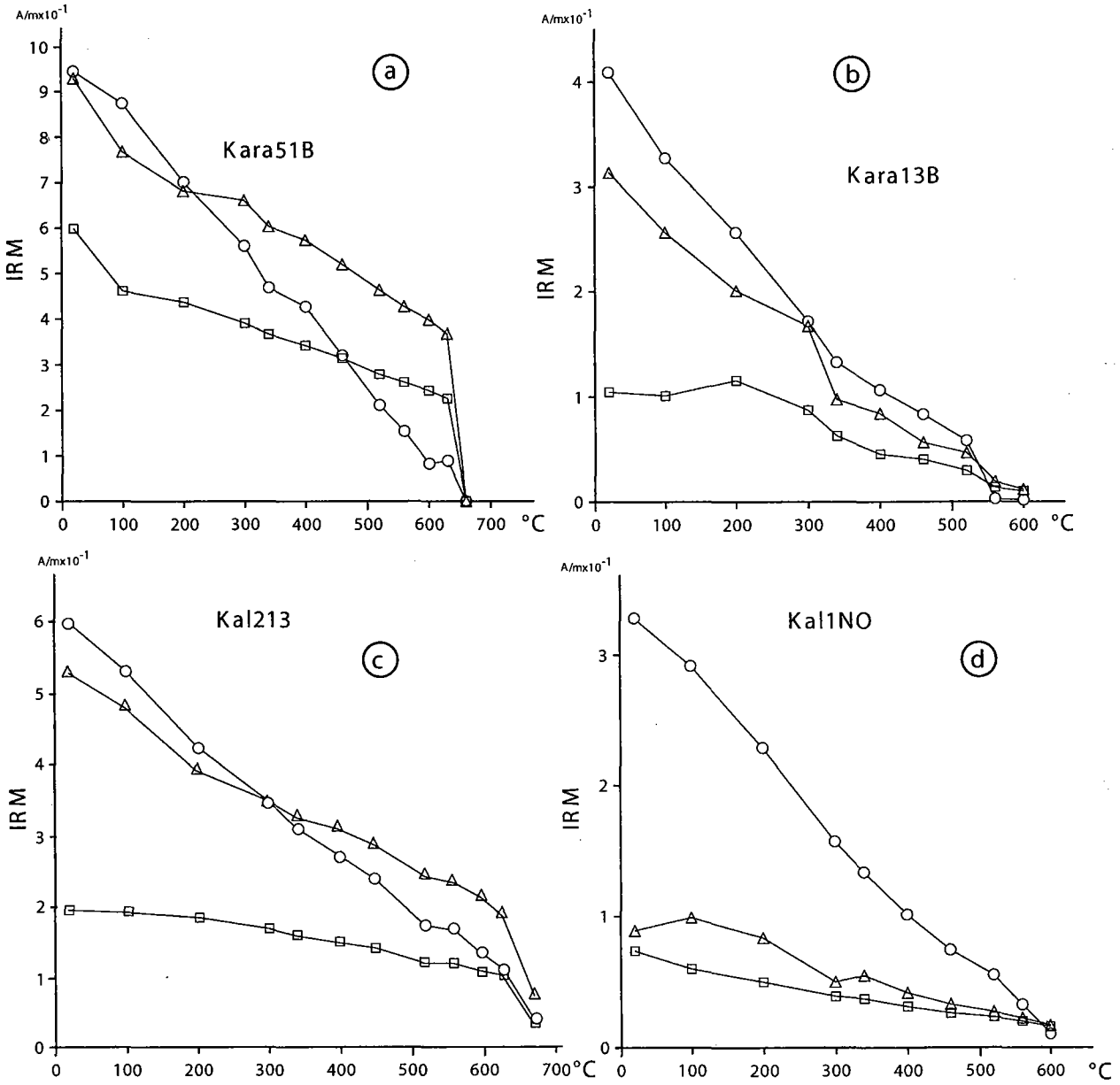

Fig. 3. IRM intensity decay during thermal demagnetization (Zaisan basin). Symbols: squares = high-coercivity component; triangles = intermediate-coercivity component; dots = low-coercivity component.

respectively. Thermal demagnetization of the IRM components clearly showed that these differences were systematically related to the ferromagnetic minerals content. In the specimens of the first group, the high- and intermediate-coercivity components regularly decreased with increasing temperature and were completely removed above 640 °C (Fig. 3a), whereas most of the low-coercivity component was removed below 570 °C. These results point to hematite as the main carrier of remanence, in good agreement with the behaviour observed during thermal demagnetization of the NRM. A ChRM component is present in most specimens of this group: its blocking temperature spectrum ranges from 400 to 460 °C to the Néel temperature and its polarity is either reverse or normal (Fig. 4a,b). At some sites, large secondary components occur, characterized by low unblocking temperature, usually less than 300 °C, and direction close to the present field. This unstable remanence could be a viscous remanence carried by the low-coercivity ferromagnetic fraction. Specimens of the second group lost all their IRM below 600 °C, with a significant decrease below 350 °C (Fig. 3b). Magnetite is the main ferromagentic mineral and no hematite is present. Both thermal and AF demagnetization usually failed to isolate a stable component. Susceptibility often increased after heating at temperatures above 300–350 °C and remanence direction changed erratically at peak-field higher than 40–50 mT, often paired with an increase in intensity. However, NRM direction of seven specimens from sites Acho1 and Acho2, which are located close to one another, showed a more regular behaviour. Their demagnetization paths defined great circles and were interpreted (Fig. 5) using the convergence method of Halls (1976). In conclusion, in the northern Zaisan basin a ChRM was successfully isolated by thermal demagnetization only in hematite-bearing rocks.

The analysis of the rock magnetic fabric was performed using AMS measurements and provided further information. The magnetic fabric is defined by the three principal susceptibilities (maximum, k_1>intermediate, k_2>minimum, k_3) and the direction of the corresponding axes, which are orthogonal to each other. The k_1 and k_2 axes define the magnetic foliation plane (Tarling and Hrouda, 1993). In the case of hematite, they lie in the basal plane and hence within the largest dimension of the grains. Hematite flakes preferentially deposit parallel to the bedding and therefore primary magnetic fabric of hematite-bearing sediments is characterized by a well-developed foliation close to the bedding plane. At sites of the first group, where hematite is the main ferromagnetic mineral, the fabric was well defined. The degree of anisotropy $P=k_1/k_3$, which gives the degree of preferred orientation, varied in the range 1.020 to 1.050. The k_3 axes always clustered close to the vertical, while k_1 and k_2 were

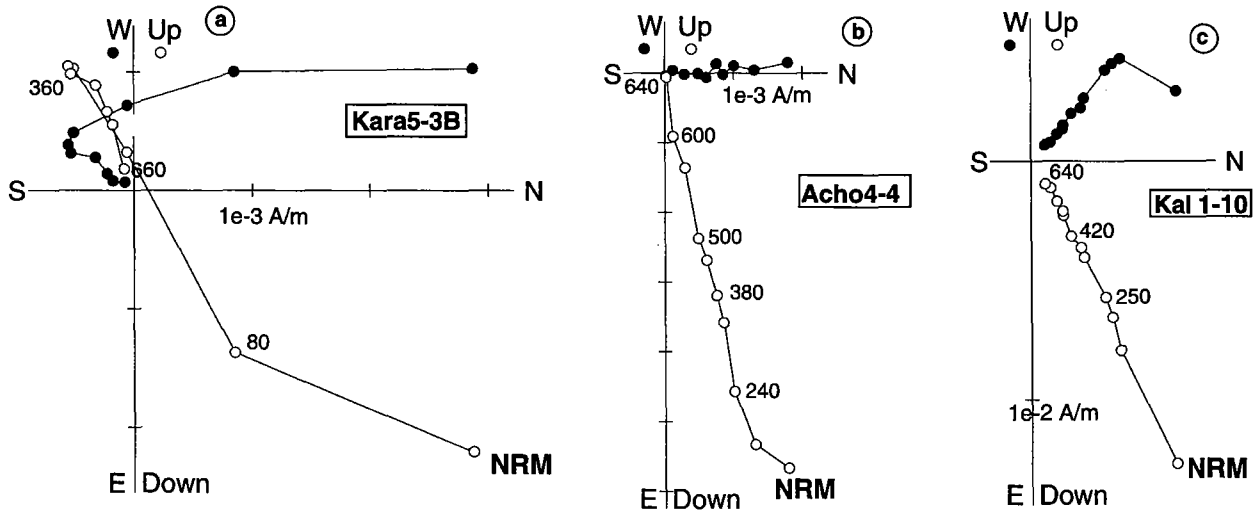

Fig. 4. Zijderveld diagrams for thermal demagnetization (Zaisan basin). Symbols: full/open dots = horizontal/vertical component; figures = temperature value (°C).

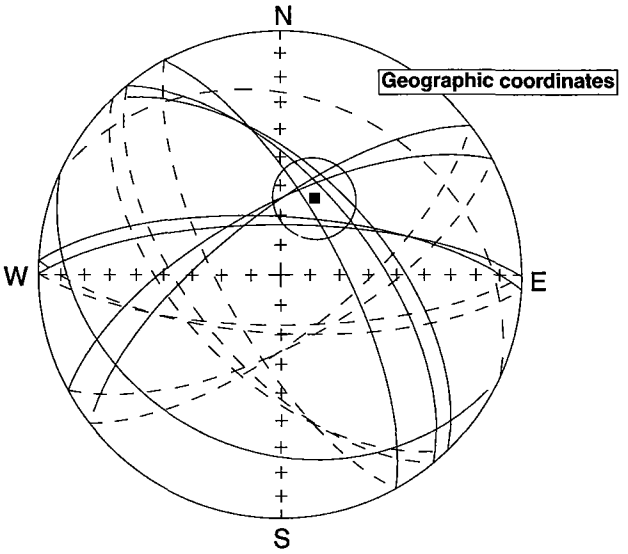

Fig. 5. Great circles analysis for sites Acho1 and Acho2 (Zaisan basin). Square = best fit for great circles intersection with 95% confidence ellipse.

either grouped or dispersed within the magnetic foliation, which lay close to the bedding (Fig. 6a). Consistency between magnetic fabric and bedding shows that the rock still preserves its primary fabric (Tarling and Hrouda, 1993 and references therein) and suggests the detrital origin of hematite, and hence the primary origin of its stable magnetization. In the sites of the second group, which yielded poor paleomagnetic results, the principal susceptibility directions were more scattered (Fig. 6b) than in the first group, the values of the anisotropy degree were lower ($P<1.020$) and the magnetic foliation differed from the bedding plane.

3.2.2. Southern border of the basin

The rocks sampled at Kalmakpay have homogeneous magnetic properties. Susceptibility varied in the range $200<k<500\times10^{-6}$ SI except at site Kal1 where it was systematically higher ($500<k<900\times10^{-6}$ SI). Thermal demagnetization of the IRM showed a high-coercivity component removed at temperatures higher than 660 °C and a low-coercivity component, which gradually decreased in intensity. Usually, the soft magnetization was greatly reduced at 600 °C and completely removed at higher temperatures (Fig. 3c). Only in some specimen from site Kal1 were all three coercivity components removed within 600 °C (Fig. 3d). Both hematite and magnetite therefore are present at Kalmakpay and their relative content varies from site to site. Thermal demagnetization proved to be more effective than AF in isolating the ChRM. A weak, low-temperature component close to the present field was removed in the first steps (Fig. 4c). Then, at sites Kal1, 2, 4, 7, a stable ChRM of either normal or reverse polarity was isolated. A well-defined magnetic fabric was observed. The principal susceptibility axes were grouped and the magnetic foliation was always close to the bedding (Fig. 6c), likely indicating a depositional origin of the magnetic fabric. No stable component could be isolated at the other three sites (Kal3, 5, 6), where the rock consisted of sandy clays, and NRM was weaker.

3.3. Paleomagnetic directions

The stable ChRM direction of each specimen was calculated using linear regression techniques and the mean site value was obtained following Fisher's statistics, with the exception of sites Acho1, 2 where the Halls' (1976) method was used. The mean site directions are listed in Table 1 and shown in the equal-area projections of Fig. 7. Mean direction calculated for the southern part of the basin is $D=176°$, $I=80°$ ($k=7$, $\alpha_{95}=36°$) in geographic coordinates and $D=0°$, $I=53°$ ($k=38$, $\alpha_{95}=15°$) after untilting, and fold test is positive at the 95% level (McFadden and Jones, 1981). For the northern part of the basin, we obtain $D=25°$, $I=59°$ ($k=20$, $\alpha_{95}=15°$) in geographic coordinates and $D=16°$, $I=63°$ ($k=15$, $\alpha_{95}=18°$) after untilting. Fold test is nonsignificant but inclinations of bedding are very low. Positive fold test for the northern part of the basin and also at the basin scale (Table 1) suggest that ChRM is prefolding. Furthermore, normal and reverse polarities occur with a positive reversal test (McFadden and Lowes, 1981) in both localities and ASM data suggest a primary magnetic fabric. We therefore conclude that the ChRM is likely as primary. The directions for the northern and southern parts of the Zaisan basin are statistically indistinguishable and suggest that they behave as a single rigid block. Indeed, there is no evidence of significant internal deformation between the two parts (Delvaux et al., submitted for publica-

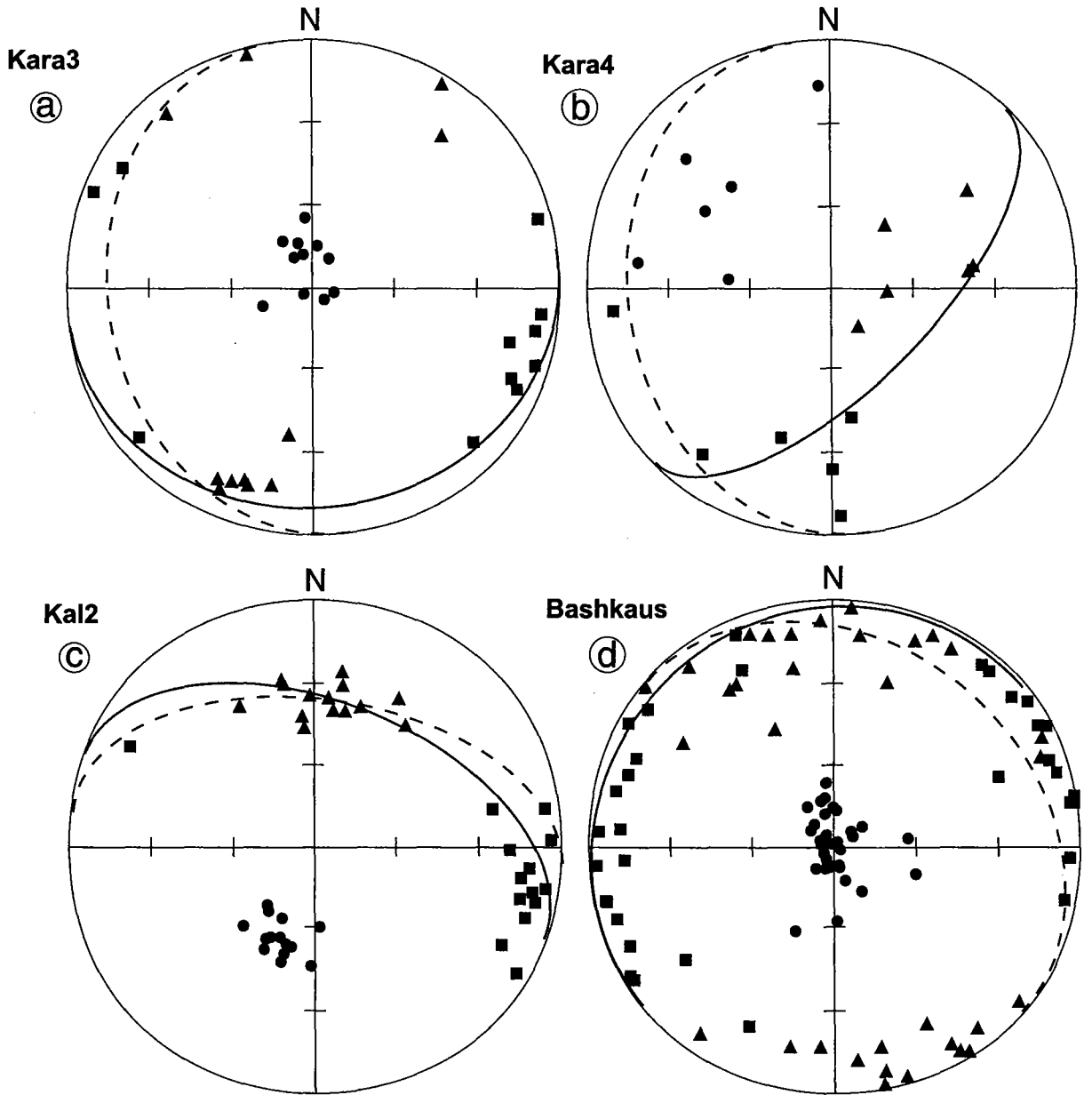

Fig. 6. Equal-area projection of the principal susceptibility axes (Zaisan and Chuya). Symbols: squares = k_1; triangles = k_2; dots = k_3; full/dashed great circles = magnetic foliation/bedding.

tion). The mean direction for the whole Zaisan basin is, after untilting, $D=9°$, $I=59°$ ($k=19$, $\alpha_{95}=11$).

4. Paleomagnetism of the Chuya depression

4.1. Stratigraphy and sampling

Several stratigraphic schemes for the Cenozoic–Quaternary sedimentary sequence of the Chuya depression were proposed in the 1960s (see Deviatkin, 1965; for a review, Zykin and Kazansky, 1995) and were recently refined on the basis of new data (Zykin and Kazansky, 1996). Basically, the sequence consists of seven units mainly composed of detrital continental sediments whose deposition started during the middle Oligocene. The total thickness in the center of the depression reaches 1 km. The sampling sites are located along the western border (Fig. 8), and about 200 specimens were collected with the same proce-

Table 1
Paleomagnetic data from the Cenozoic sediments of the Zaisan basin

Site	Age	Latitude (°N)	Longitude (°E)	Bedding, dd/dip	*n/N*	*D*	*I*	D_c	I_c	*k*	α_{95}
North Zaisan											
Kara3	L. Eocene	84.4	48.1	250/15	12/13	230	−45	218	−57	7	18
Kara5	Paleocene	84.4	48.1	250/15	6/11	208	−70	161	−74	27	13
Acho1–2 (GC)	U. Paleocene–L. Eocene	84.2	48.1	196/20	7/20	024	62	027	82		14
Acho4	Oligocene	85.3	48.0	0/0	15/15	008	73	008	72	50	5
Acho5	U. Paleocene–L. Eocene	85.3	47.9	6/5	6/7	031	34	030	30	49	10
Acho6	U. Paleocene–L. Eocene	85.3	47.9	6/5	6/9	171	−60	173	−55	44	10
Mean North Zaisan					6	025	59			20	15
								16	63	15	18
South Zaisan											
Kal1	Miocene	85.4	47.3	21/35	9/15	316	78	004	49	13	15
Kal2	Oligocene	85.4	47.3	–	6/10	148	78	023	60	20	15
Kal4	Oligocene	85.4	47.3	16/35	6/7	147	−78	183	−46	31	12
Ka17	Paleocene	85.4	47.3	335/89	6/10	346	−38	154	−53	36	11
Mean South Zaisan					4	176	80			7	36
								0	53	38	15
North + South Zaisan		85.4	47.3		10/10	032	74			8	19
								9	59	19	11

Symbols: GC = ChRM direction calculated using great circles convergence method; Bedding: dd = dip direction, dip = inclination of the bedding (bedding is not indicated when different between cores at one site); *n/N* = number of successfully demagnetized/collected specimens; *D*, *I* = declination, inclination; D_c, I_c = declination, inclination after tilt correction; *k* = Fisher's precision; α_{95} = semiangle of confidence.

dure as in the Zaisan basin. The mean magnetic declination was 5°.

A white weathering crust derived from the alteration of a deformed Paleozoic basement usually occurs at the base of the sequence (Fig. 8). It is overlaid by the middle–upper Oligocene Karachum unit (1), which mainly consists of subaerial kaolin clays, brown to red in color. This unit is up to 40-m

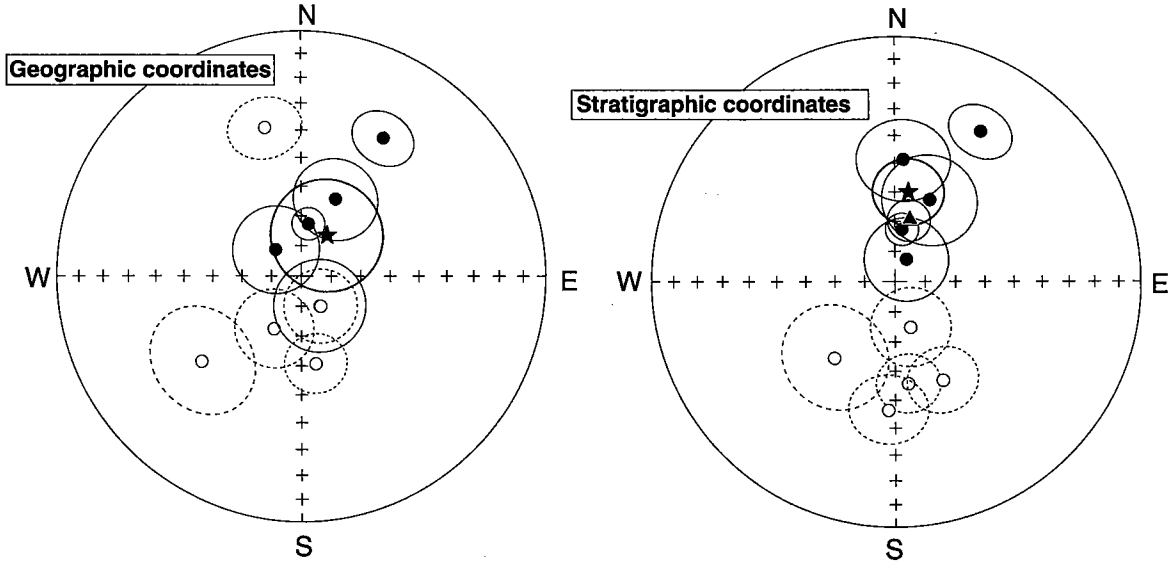

Fig. 7. Equal-area projection of mean site ChRM directions and associated 95% confidence ellipses for the Zaisan basin. Symbols: full/open dots = normal/reverse polarity; star = mean direction; triangle = expected direction at 40 Ma from the APW path of stable Asia (Besse and Courtillot, 1991).

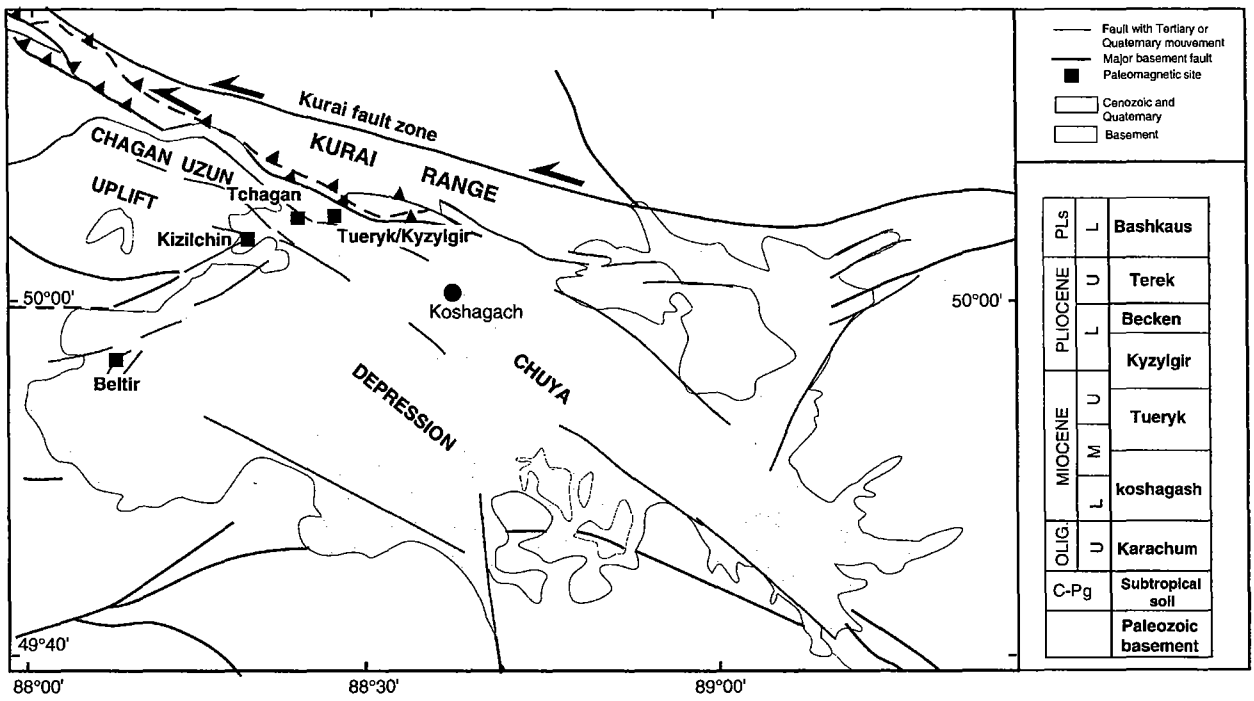

Fig. 8. Structural sketch of the Chuya depression (simplified from Delvaux et al., 1995) and location of sampling sites.

thick and deposited in a shallow lacustrine basin during dry climate conditions. Specimens were collected at one locality inside the basin (Tchagan) and another close to its margin (Kizilchin). The Koshagach unit (2) is early–middle Miocene in age and up to 250-m thick. It is made of brown, green and dark clays, aleurites and fine-grained sands with lenses of coal. The Tueryk unit (3) is composed of green-grey coloured, fine lacustrine clays. Its age is middle–upper Miocene and its thickness about 150 m. The samples were collected from an escarpment along the right bank of the Tueryk river. The late Miocene to early Pliocene age of the Kyzylgir unit (4) is well defined by abundant fossil remains: 63 species of freshwater mollusks have been found together with ostracods, fishes, mammals (*Hipparion*) and plants (Zykin and Kazansky, 1995). It is composed of yellow to brown sands with levels of stromatolite limestone. This unit deposited in a long-lived deep lake and its total thickness is about 100 m. The lower Pliocene Beken unit (5) is made of green muds and fine sandstones with lenses of coarse and poorly sorted gravel, which point to the beginning of the main uplift phase. The Terek and Bashkaus units (6–7) are molassic-type sediments with sandstones levels, deposited during the strong tectonic activity, which resulted in the uplift of the adjacent ranges during late Pliocene and early Pleistocene.

4.2. Magnetic measurements

Measurements were performed in the same way as for the Zaisan basin samples. The results are presented separately for each sedimentary unit because of their heterogeneous magnetic properties.

4.2.1. Karachum unit

Magnetic susceptibility varied between sites: it was of the order of $100–200 \times 10^{-6}$ SI at Kizilchin, whereas at Tchagan its value was higher and reached $500–900 \times 10^{-6}$ SI. The magnetic fabric was usually poorly defined, owing to the dispersion of the principal susceptibility axes. The NRM intensity was of the order of 10^{-3} A/m. It consisted of a low-temperature component, removed after heating at 350–400 °C (Fig. 9a) and either clustered near the present field or strongly scattered, and a high-temperature component of normal or reverse polarity completely removed at temperatures higher than 660 °C. This behaviour is consistent with the results of the

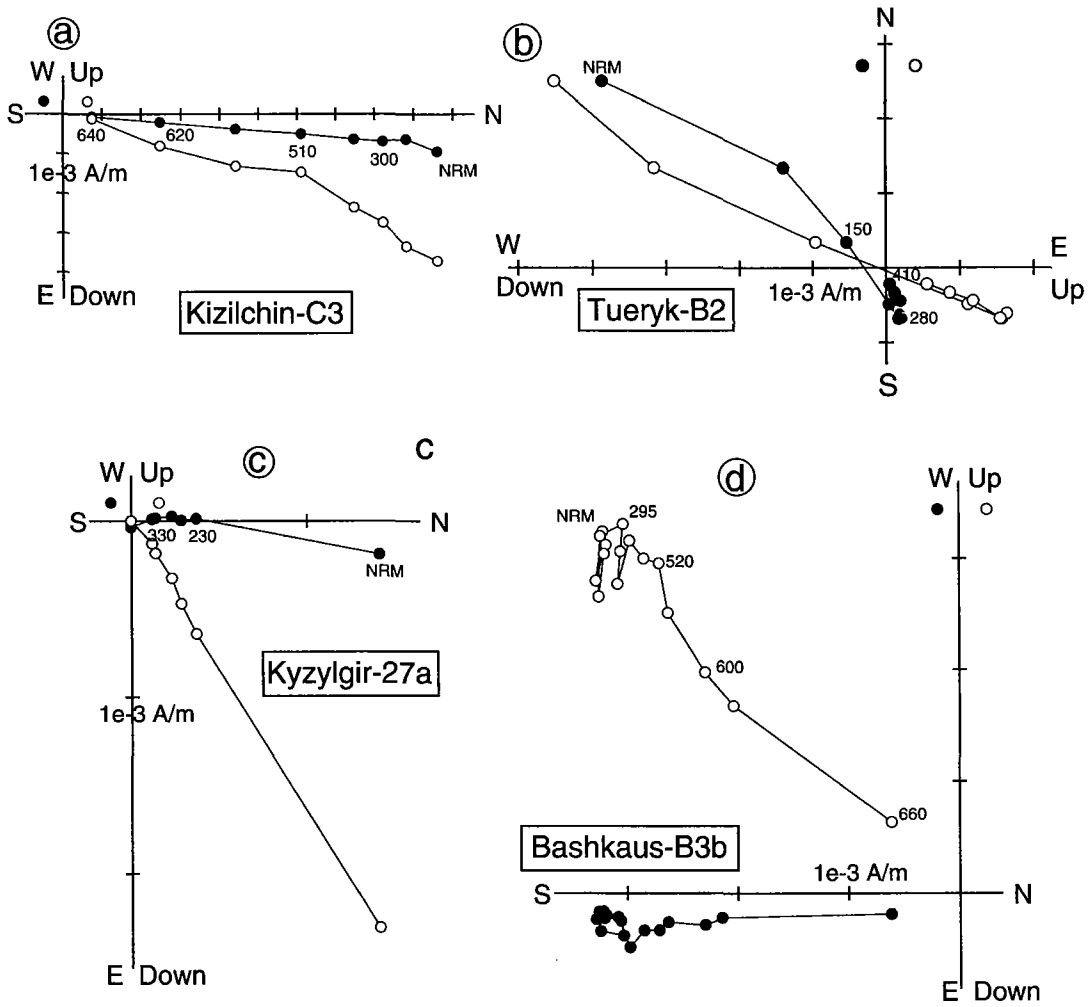

Fig. 9. Zijderveld diagrams for thermal demagnetization (Chuya depression). Same symbols as in Fig. 4.

thermal demagnetization of the IRM. The strong decrease below 500 °C (Fig. 10a) points to the presence of magnetite, and the fraction that persists at higher temperatures is carried by hematite. The high-temperature component carried by hematite was successfully isolated in about half of the specimens from the TchaganA, TchaganD and KizilchinC sites. At TchaganC, a characteristic component was isolated using the great circles convergence method (Halls, 1976).

4.2.2. Tueryk and Kyzylgir units

The specimens of the Tueryk unit were collected in stratigraphical order from a 20-m-high escarpment. Susceptibility varied from 200 to 500×10^{-6} SI, and was higher in the lower part of the section. The magnetic fabric was well defined, characterized by a magnetic foliation close to the bedding. The IRM thermal demagnetization showed (Fig. 10b) a magnetization carried by low to intermediate coercivity minerals, which decreased sharply from room temperature to 350 °C and was completely removed at 450 °C. These results suggest that the NRM is carried by an iron sulfide together with magnetite. The NRM had intensity in the range 10^{-2} to 10^{-3} A/m and always consisted of two components (Fig. 9b), one unstable, completely removed at 200–250 °C and whose polarity was normal, and the other one stable up to 400–410 °C. In two-thirds of the specimens, stepwise thermal demagnetization was successful in isolating a stable ChRM whose polarity was normal in the upper and middle part of the section, reverse in the lower part.

The magnetic characteristics of the Kyzylgir unit were similar. A low-temperature magnetization com-

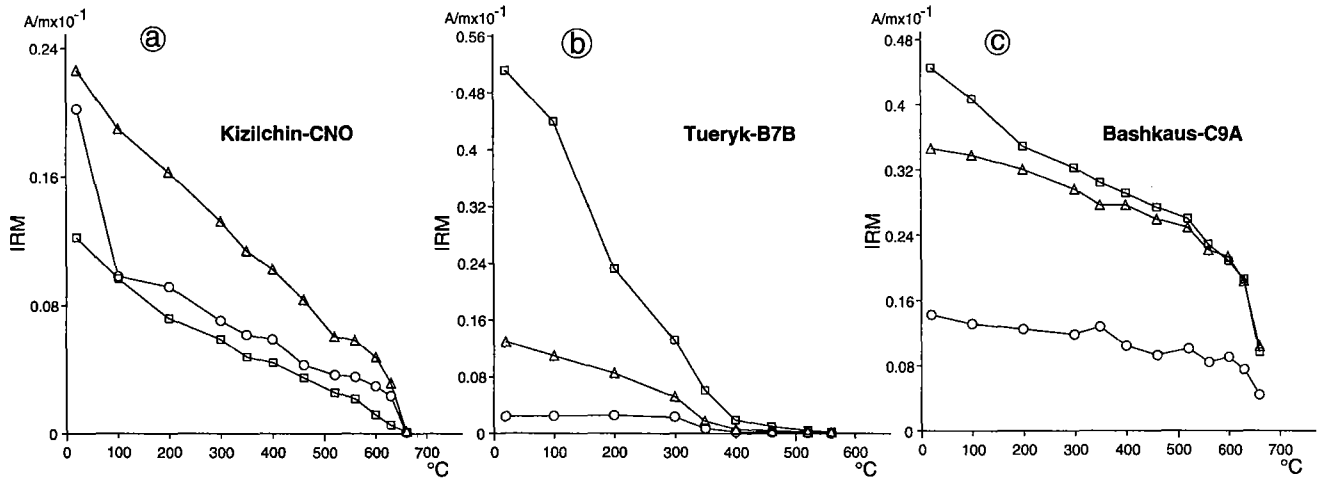

Fig. 10. IRM intensity decay during thermal demagnetization (Chuya depression). Same symbols as in Fig. 3.

ponent (Fig. 9c) was removed by thermal demagnetization up to 180 °C. A ChRM component with normal polarity was isolated in the range 230 to 420 °C and completely removed at 450 °C.

4.2.3. Bashkaus unit

The magnetic properties were similar in all specimens. Susceptibility varied in the range 200 to 300×10^{-6} SI. The fabric was very well developed and strongly foliated. The values of the anisotropy degree varied from 1.050 to 1.100 and the magnetic foliation coincided with the bedding (Fig. 6d). Thermal demagnetization of both IRM and NRM unambiguously showed that hematite is the main carrier of magnetization. The high-, intermediate- and low-coercivity IRM components (Fig. 10c) decreased slowly up to 600 °C and were then removed in the range 650 to 670 °C. The intensity of the NRM was of the order of 10^{-2} A/m and the polarity of ChRM either normal or reverse. Secondary components were negligible: direction was stable throughout demagnetization and the NRM completely removed at temperatures higher than 660 °C (Fig. 9d).

4.3. Paleomagnetic directions

We obtained reliable ChRM directions from the Tueryk, Kyzylgir and Bashkaus units (Table 2). For the Karachum unit, within- and between-site dispersion was rather high and only four sites out of nine did provide reliable ChRM. The Karachum data were therefore not used for further analysis. We combined the results from the Tueryk and Kyzylgir units since their ages do not differ much and the sites are close to each other. Their mean direction in geographic coordinates is $D=340°, I=62°$ ($k=27, \alpha_{95}=4°$) (Fig. 11a).

Table 2
Paleomagnetic data from the Cenozoic sediments of the Chuya depression

Site	Unit	Age	Latitude (°N)	Longitude (°E)	Bedding, dd/dip	*n/N*	*D*	*I*	D_c	I_c	*k*	α_{95}
TchaganA	Karachum	U. Oligocene	88.3	50.1	0/0	6/16	346	60	346	60	14	18
TchaganC (GC)	Karachum	U. Oligocene	88.3	50.1	0/0	6/9	322	8	322	8		11
TchaganD	Karachum	U. Oligocene	88.3	50.1	0/0	8/12	343	36	343	36	6	24
KizilchinC	Karachum	U. Oligocene	88.2	50.1	320/10	6/11	353	31	350	23	13	19
Tueryk	Tueryk	U. Miocene–U. Plioc.	88.4	50.1	180/05	26/39	330	60	330	60	25	6
Kyzylgir	Kyzylgir	M.–U. Miocene	88.2	50.1	210/12	20/22	000	62	342	67	80	4
Tueryk+Kyzylgir						46/61	340	62			27	4
									332	63	31	4
Beltir	Bashkaus	Pleistocene	88.1	49.9	–	16/24	001	54	009	46	25	7

Same symbols as in Table 1.

Bedding is nearly horizontal at Tueryk and gently dips northwards at Kyzylgir. After tilt correction, the mean direction is $D=332°$, $I=63°$, with slightly better clustering ($k=31$, $\alpha_{95}=4°$). The lower part and the middle to upper part of the Tueryk section provided reverse and normal polarity, respectively. This suggests that two polarity chrons were sampled, but it is not enough to affirm a primary origin of the ChRM since the reversal test was not significant. However, the deviation of the ChRM direction with respect to the present field is significant and bears witness that these units were tectonically displaced after their remanence, whichever its origin, was acquired.

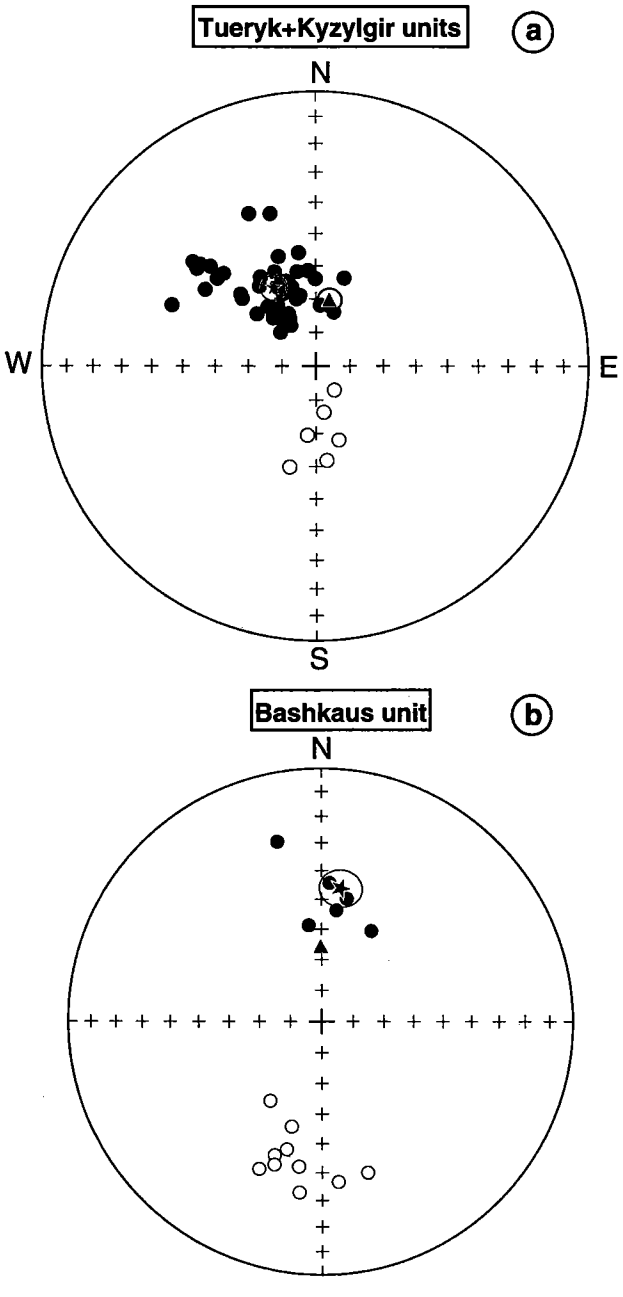

Fig. 11. Equal-area projection of the single specimen ChRM directions for the Chuya depression. Same symbols as in Fig. 7. The triangles are the expected directions for stable Asia, present field for the Bahskaus unit and at 20 Ma (Besse and Courtillot, 1991) for Tueryk and Kyzylgir units.

The mean direction for the Bashkaus unit in geographic coordinates is $D=1°$, $I=54°$ ($k=25$, $\alpha_{95}=7°$). Both normal and reverse polarities occurred (Fig. 11b), and the reversal test (McFadden and Lowes, 1981) was positive at the 99% confidence level. Fold test was not possible as bedding is uniform at the Beltir site where the Bashkaus unit was sampled. After untilting, the mean direction is $D=9°$, $I=46°$ ($k=25$, $\alpha_{95}=7°$). The inclination value is much lower than expected at the site latitude for the Pleistocene magnetic field ($I=67°$). This difference may be interpreted as an inclination shallowing due to the depositional geometry, as shown by the strong magnetic foliation. It is typical of detrital remanence (DRM) and has been well documented in hematite-bearing sediments similar to the sands sampled at Beltir (Tauxe and Kent, 1984; Rösler et al., 1997). Both fabric and remanence characteristics point therefore to a primary origin for the ChRM of the Bashkaus unit.

5. Paleomagnetic directions and rotation pattern in the Altai-Zaisan domain

We compared our directions with the reference directions for stable Asia derived from the APW path of Besse and Courtillot (1991). For the Zaisan basin, we referred to the direction at 40 Ma, since the APW path do not show substantial variations from Paleocene to Miocene. The Zaisan basin direction ($D=9°$, $I=59°$, $k=19$, $\alpha_{95}=11°$) is close to that expected for stable Asia ($D=14\pm6°$, $I=69°\pm7°$), with a slightly lower inclination. The differences between the measured and reference values are not statistically significant: $R=5\pm22°$ and $F=10\pm10°$ for declination and inclination, respectively (Beck, 1980; Demarest, 1983). Paleomagnetic data therefore show no rotation of the Zaisan basin relative to stable Asia during the Cenozoic. For the Chuya depression, we referred the

Tueryk and Kyzylgir units to the direction at 20 Ma, and the Bashkaus unit to the present field as no significant motion of the Eurasian plate occurred during the Quaternary. The paleomagnetic direction from the Bashkaus unit ($D=9°$, $I=46°$, $k=25$, $\alpha_{95}=7°$) is consistent with the expected declination ($D=0°$, $I=67°$) but inclination is significantly different ($R=9\pm8°$ and $F=21\pm6°$, respectively). In the previous section, we interpreted this difference as an inclination shallowing related to depositional fabric. The middle Miocene to early Pliocene paleomagnetic direction from the Tueryk and Kyzylgir Units ($D=332°$, $I=63°$, $k=31$, $\alpha_{95}=4°$), on the other hand, differs from the reference direction ($D=11\pm5°$, $I=70\pm2°$). Inclination is not far from the expected value ($F=7\pm4°$), whereas declination is strongly deviated ($R=39\pm8°$). These data suggest a counterclockwise rotation of the Chuya depression relative to stable Asia of at least 30° since late Miocene–early Pliocene. As previously described, the Chuya depression developed during late Tertiary in a left-lateral transpressional context. The North Chuya and the Kurai faults (Fig. 8), which bound the depression to the north, are indeed typical flower structures accommodating left-lateral displacement (Delvaux et al., submitted for publication). We suggest that left-lateral shear induced counterclockwise rotation of the Chuya depression in a domino style. No other paleomagnetic data are available for the Altai domain, but structural evidence supports counterclockwise rotations for the whole Altai range. Detailed kinematic studies of faults systems of the Mongolian Altai (Bayasgalan et al., 1999) based on field and earthquake data indicates that right-lateral strike-slip faults oriented NW–SE terminate to the northwest with E–W to N100° oriented thrust, along which displacement decreases away from the fault (Fig. 12). This style of faulting also implies counterclockwise rotation of the whole deformation zone, and the whole western Altai, according to Bayasgalan et al. (1999), has experienced counterclockwise rotation about a vertical axis. Hence, paleomagnetic rotations, although restricted to a small area, may be representative of the western Altai domain. Lastly, structural data on the Chuya depression (Delvaux et al., submitted for publication) indicate that regional tectonics intensified in the late Pliocene–early Pleistocene. Rotation is therefore recent and probably occurred during the last 5 million years.

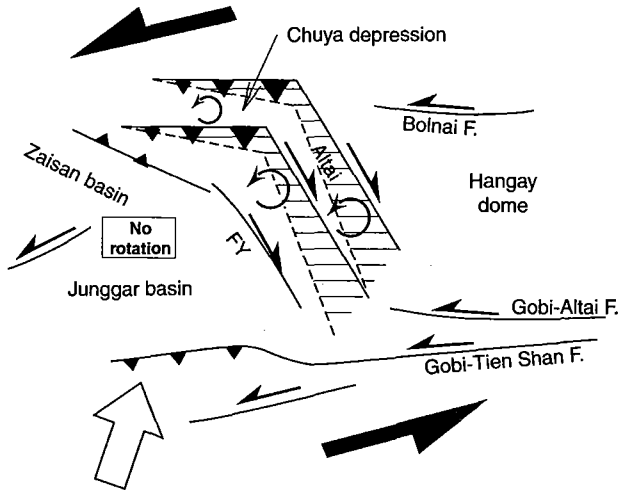

Fig. 12. Tectonic scheme for the Altai-Zaisan domain. Open arrow indicates the orientation of the maximal horizontal stress. See text for further explanation.

To understand the mechanisms controlling rotations in the Altai, one should consider the boundary conditions controlling deformation in Mongolia. Considerable evidences of major left-lateral faulting have been reported and studied in detail from field and seismotectonic data (Baljinnyam et al., 1993; Cunningham et al., 1996b; Cunningham, 1998; Bayasgalan et al., 1999). In northern Mongolia, the left-lateral Bolnai fault (Figs. 1 and 12) is more than 500-km long and shows important historical seismicity with magnitude of earthquakes greater than 7.0. South of the western Altai, important historical seismicity has occurred in several major belts of left-lateral transpression comprising the Gobi-Altai and the Gobi-Tien-Shan faults systems (Figs. 1 and 12). This corridor is considered as the easternmost extension of a broad belt of left-lateral shear, which extends from the Pamirs to Mongolia and the Baikal (Cobbold and Davy, 1988; Cunningham, 1998). Left-lateral shear therefore appears as one of the main boundary condition controlling deformation in western Mongolia, within a maximum horizontal stress roughly oriented N30 (Cunningham, 1998). We infer that, within this shear zone and especially in the Altai, block bounded by antithetic right lateral faults have rotated counterclockwise in a domino fashion. (Fig. 12). Further to the east, although the Hangay dome probably disturbed the tectonic regime in Central

Mongolia (Cunningham, 1998), left-lateral shear likely also prevailed since paleomagnetic data indicate counterclockwise rotations of up to 30° in eastern Mongolia (Fig. 13) (Pruner, 1987).

Conversely, no rotation are observed to the west in the Zaisan and Junggar basins with a sharp discontinuity along the western border of the Altai, corresponding to the Irtysh/Fu-Yun fault zone (Figs. 12 and 13). As the regional maximum horizontal stress is homogenous (Cunningham, 1998), the changing pattern of rotations between the Altai and Zaisan-Junggar domains implies different styles of deformation and faulting. This could reflect a partitioning of the deformation, which accommodates the regional left-lateral shear, dominantly compressive in the Junggar–Zaisan domain and dominantly transpressive in the Altai.

6. Discussion

The available paleomagnetic data representative of the Cenozoic deformation for northern central Asia are reported in Table 3 and Fig. 13. They include Cenozoic and Cretaceous data since the Cretaceous deformation in northern central Asia is essentially related to the India–Asia collision (Enkin et al., 1992; Chen et al., 1993; Halim et al., 1998). The pattern of vertical axis rotations appears complex and heterogeneous within the Pamirs–Baikal strip and several domains of rotations may be distinguished from SW to NE. Large rotations up to 70° are observed in and along the Pamirs range, clockwise to the east and counterclockwise to the west. They have been related to oroclinal bending in the western Himalayan syntaxis (Bazhenov and Burtman, 1986;

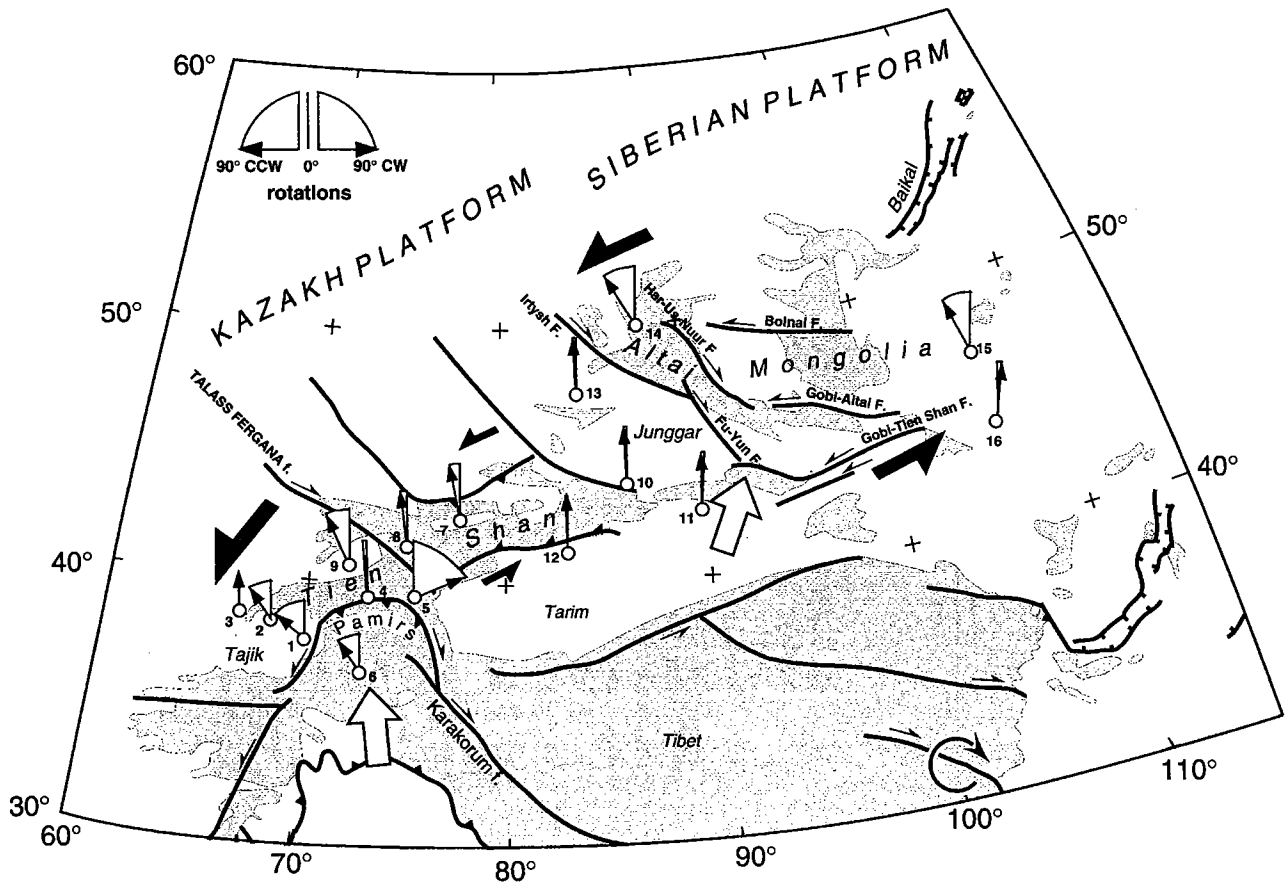

Fig. 13. Paleomagnetic rotations from Cretaceous and Cenozoic rocks in northern central Asia (numbers refer to Table 3). Black half arrows indicate shear within the left lateral Pamirs–Baïkal wrenching strip. Their size is proportional to magnitude of shear within the strip. The open arrows indicate the orientation of maximum horizontal stress for the Altai domain (Cunningham, 1998).

Table 3
Selected Mesozoic and Cenozoic paleopoles within the Pamirs–Baïkal strip

Domain	No.	Area	Age	Site		Paleopole		dp/dm, A95	Rotation/ Eurasia	Reference
				Latitude	Longitude	Latitude	Longitude			
Eurasia (APWP)										
130–65Ma						76.3	202.6	2.2		Enkin et al. (1992)
40 Ma						80.2	145.4	3.8		Besse and Courtillot (1991)
20 Ma						82.3	147.6	3.2		Besse and Courtillot (1991)
Pamirs	4	North central	P	39.0	70.0	59.1	317.5	5/9	$47 \pm 9°$	Bazhenov and Burtman (1986)
	5	Northeast	P	39.4	74.0	50.5	174.0	6/10	$-27 \pm 10°$	Bazhenov and Burtman (1986)
	6	Chitral	E	36.5	72.3	36.1	135.3	3/6	$61 \pm 7°$	Klootwijk et al. (1994)
Tajik basin	1	South Darvaz	E–O–M	37.8	68.2	43.4	325.8	7/12	$59 \pm 10°$	Thomas et al. (1994)
	2	Pyryagata	M	37.7	68.1	59.7	299.0	7/13	$35 \pm 12°$	Thomas et al. (1994)
		Pulkhakim	M	38.0	67.4	69.0	277.6	8/15	$21 \pm 13°$	Thomas et al. (1994)
	3	Dekhanabad	M			67.0	239.0	5/9	$7 \pm 9°$	Chauvin and Perroud (1996)
Tien-Shan range	7	Issik–Kul	E–O–M	42.3	76.7	78.0	250.0	5/8	$11 \pm 9°$	Thomas et al. (1993)
	8	Naryn	P	41.0	74.0	69.0	241.7	8/13	$8 \pm 11°$	Thomas et al. (1993)
	9	Fergana	O–M	41.3	72.2	62.7	241.7	6/10	$31 \pm 10°$	Thomas et al. (1993); Bazhenov (1993)
Junnggar basin	10	Manas	K	44.2	86.0	73.4	223.6	4.3	$2 \pm 6°$	Chen et al. (1991)
Turfan depression	11		K	43.0	90.0	65.1	227.8	5/8	$2 \pm 8°$	Cogné et al. (1995)
Tarim basin	12	Kuche	K	41.6	83.5	66.2	223.3	6/10	$2 \pm 9°$	Li et al. (1988)
Zaisan basin	13		P–M	48.0	84.3	79.5	222.6	12/16	$5 \pm 22°$	This paper
Altai range	14	Chuya	M–Pl	50.0	88.2	46.0	255.9	5/6	$39 \pm 8°$	This paper
Mongolian block	15	Ulan Bator	K	46.8	107.3	86.2	337.5	7/9	$23 \pm 10°$	Pruner (1987)
	15	Ulan Bator	K	46.8	107.3	80.9	12.7	8/10	$32 \pm 10°$	Pruner (1987)
	16	Gobi desert	K	43.8	107.9	72.5	204.5	6/9	$-4 \pm 9°$	Pruner (1987)

No. refers to numbers in Fig. 12. Symbols: Age = K, Cretaceous; P, Paleocene; E, Eocene; O, Oligocene; M, Miocene; Pl, Pliocene; dp/dm, A95 = confidence limit of paleopole. Rotation relative to Eurasia (Besse and Courtillot, 1991) is calculated according to Beck (1980) and Demarest (1983) and taken as positive when counterclockwise.

Klootwijk et al., 1994) and to opposite shear along the eastern and western margins of the Pamirs, right-lateral and left-lateral, respectively (Searle, 1996). North and west of the Pamirs, counterclockwise rotations up to 35° are observed in the western Tien-Shan range and in the Tajik depression (Thomas et al., 1993, 1994; Bazhenov, 1993; Bazhenov et al., 1994). Conversely, in central Tien-Shan, east of the Talass–Fergana fault, counterclockwise rotations if any are small, always less than 10°. In the Tien-Shan area, all rotations are confined to the range and did not occurred in the Kazakh platform to the north and in the Tarim basin to the south. Further to the east, no rotations are observed in the Junggar–Zaisan area (Chen et al., 1991; Cogné et al., 1995) and significant counterclockwise rotations occur in western Mongolia.

Two main points can be drawn from this pattern:

(1) boundaries between different rotation domains are sharp and correspond to major faults or faults zones (e.g. The Talass–Fergana fault or the Irtysh/Fu-Yun fault zone);
(2) rotations are always counterclockwise, except in the specific case of the Pamirs where oroclinal bending likely explains a more complicated pattern.

The consistency of the direction of rotation from the Tajik depression to Mongolia supports the hypothesis of a large left-lateral shear zone accommodating the northwestward displacement of mobile Asia relative to stable Asia. Within this zone, individual blocks bounded by antithetic right-lateral faults rotate counterclockwise (Cobbold and Davy, 1988; Cunningham, 1998). However, as already observed for the Junggar–Zaisan-Altai domain, the heterogeneous pattern of rotation also reflects heterogeneous deformation and style of faulting within the shear zone (Fig. 13). In the western Tien-Shan and the Tajik depression, large rotations are likely associated to the northward indentation of the Pamirs and the left-lateral shear it induces with respect to the Kazakh platform. East of the Talass–Fergana fault, rotations are small, indicating dominant compressive faulting with little shear component. Indeed, at a regional scale, orientation of the maximum horizontal stress implies dominant compression on major faults. To the East, the transition with the Altai is sharp and left-lateral shear component becomes dominant again. However, more paleomagnetic data in the Mongolian territory are needed to test the extension of the left-lateral shear to the east and the influence of the Hangai dome on the regional kinematics.

7. Conclusions

We presented new paleomagnetic data on Tertiary rocks from southeastern Kazakhstan (Zaisan basin) and the Siberian Altai (Chuya depression). The results from the Zaisan basin are consistent with those from the Junggar basin to the south and do not show either significant latitudinal displacement or vertical axis rotation relative to stable Asia. Those from the Chuya depression reveal a Tertiary counterclockwise rotation of $39 \pm 8°$ relative to stable Asia. This rotation is supported by independent geological data and likely reflects rotations of the whole Altai. A sharp variation in the tectonic style between the Junggar–Zaisan domain and the Altai range is proposed to explain the different rotation pattern, which could be related to a partitioning of the deformation accommodating convergence between India and Asia. The paleomagnetic data from northern central Asia demonstrate that block rotations around a vertical axis can be an important mechanism accommodating Cenozoic deformation. The pattern of rotations supports the hypothesis of a left-lateral shear zone running from the Pamirs to the Baikal. Different amounts of rotation, however, reflect varying degree of shear, in relation with local boundary conditions.

Acknowledgements

This work was carried out in the frame of the CEE-INTAS program RIFT-CASIMIR no. 93-134. J.-C.T. and R.L. gratefully acknowledge additional grants by the French Embassy in Russia and the Italian CNR, C.S. Geodinamica delle Catene Collisionali. J.P. Cogné kindly provided his paleomagnetic software PALEOMAC. D. Delvaux is working in the frame of programme TECTORIFT of the SSTC, Belgian State (Services du Premier Ministre-Services fédéraux des affaires scientifiques, techniques et culturelles). This

Houseman, G., England, P., 1986. Finite strain calculations of continental deformation: 1. Method and general results for convergent zones. J. Geophys. Res. 91 (B3), 3651–3663.

Houseman, G., England, P., 1993. Crustal thickening versus lateral expulsion in the Indian–Asian continental collision. J. Geophys. Res. 98, 12233–12249.

Huang, K., Opdike, N.D., 1992. Paleomagnetism of Cretaceous to lower Tertiary rocks from southwestern Sichuan: a revisit. Earth Planet. Sci. Lett. 112, 29–40.

Klootwijk, C.T., Conaghan, P.J., Nazirullah, R., de Jong, K.A., 1994. Further paleomagnetic data from Chitral (Eastern Hindukush): evidence for an early India–Asia contact. Tectonophysics 237, 1–25.

Li, Y., Zhang, Z.K., McWilliams, M., Sharps, R., Zhai, Y.J., Li, Y.A., Li, Q., Cox, A., 1988. Mesozoic paleomagnetic results of the Tarim craton: Tertiary relative motion between China and Siberia? Geophys. Res. Lett. 15, 217–220.

Lowrie, W., 1990. Identification of ferromagnetic minerals by coercivity and unblocking temperatures properties. Geophys. Res. Lett. 17 (2), 159–162.

McFadden, P.L., Jones, D.L., 1981. The fold test in paleomagnetism. Geophys. J. R. Astron. Soc. 67, 53–58.

McFadden, P.L., Lowes, L., 1981. The discrimination of mean direction drawn from fisherian distributions. Geophys. J. R. Astron. Soc. 67, 19–33.

Mekhed, L.P., Chamikov, I.F., 1987. Techniques and results of reconnaissance seismic surveys in the zaisan basin. Isvestia Akd. Nauk. Kasakh SSR, Ser. Geologycheskaya 5, 80–87.

Molnar, P., Tapponnier, P., 1975. Cenozoic tectonics of Asia: effects of a continental collision. Science 189, 419–426.

Pruner, P., 1987. Paleomagnetism and paleogeography of Mongolia in the Cretaceous, Permian and Carboniferous–Preliminary data. Tectonophysics 139, 155–167.

Rösler, W., Metzler, W., Appel, E., 1997. Neogene magmatic polarity stratigraphy of some fluviatile Siwalik sections, Nepal. Geophys. J. Int. 130, 89–111.

Searle, M.P., 1996. Geological evidence against large-scale pre-Holocene offsets along the Karakoram fault: implications for the limited extrusion of the Tibetan plateau. Tectonics 15, 171–186.

Tapponnier, P., Molnar, P., 1979. Active faulting and cenozoic tectonics of the Tien-Shan, Mongolia and Baïkal region. J. Geophys. Res. 82 (20), 2905–2930.

Tapponnier, P., Peltzer, G., Armijo, R., 1986. On the mechanics of the collision between India and Asia. In: Coward, M.P., Ries, A.C. (Eds.), Collision Tectonics. Geol. Soc. Spec. Pub., pp. 115–157.

Tarling, D.H., Hrouda, F., 1993. The Magmatic Anisotropy of Rocks. Chapman & Hall, London, 217 pp.

Tauxe, L., Kent, D.V., 1984. Properties of a detrital remanence carried by hematite from study of modern river deposits and laboratory redeposition experiments. Geophys. J. R. Astron. Soc. 77, 543–561.

Thomas, J.-C., Perroud, H., Cobbold, P.R., Bazhenov, M.L., Burtman, V.S., Chauvin, A., Sadybakazov, E., 1993. A paleomagnetic study of Tertiary formation of the Kirghiz Tien-Shan and its tectonic implications. J. Geophys. Res. 98, 9571–9589.

Thomas, J.C., Chauvin, A., Gapais, D., Cobbold, P.R., Bazhenov, M.L., Perroud, H., Burtman, V.S., 1994. Paleomagnetic evidence for Cenozoic block rotation in the Tadjik depression (Central Asia). J. Geophys. Res. 99, 15141–15160.

Vasilenko, E., 1961. Geological History of the Zaisan Basin. VNIGRI, Moscow, 276 pp.

Zykin, V.S., Kazansky, A.Y., 1995. Main problems of stratigraphy and paleomagnetism of Cenozoic (prequaternary) deposits of Chuya depression of Gorno Altay. Russ. Geol. Geophys. 35, 75–90.

Zykin, V.S., Kazansky, A.Y., 1996. New data on Cenozoic deposits in the Chuya depression, Gorny Altai: stratigraphy, paleomagnetism, evolution, continental rift tectonics and evolution of sedimentary basins. Russ. Acad. Sci., Novosib., 74–75.